

Theoretical study on the two-dimensional second-order nonlinear optical properties: a series of charge-transfer covalently bonded organoimido derived hexamolybdate complexes

Y. L. Si · C. G. Liu · E. B. Wang · Z. M. Su

Received: 17 November 2008 / Accepted: 15 December 2008 / Published online: 8 January 2009
© Springer-Verlag 2009

Abstract To probe the cooperativity of charge transfer between organoimido and hexamolybdate, and enhance the second-order nonlinear optical (NLO) response of organoimido derivatives of hexamolybdates, electronic structures and second-order NLO properties of a series of charge-transfer covalently bonded organoimido derived hexamolybdate complexes with donor-(π conjugated bridge)-acceptor-(π conjugated bridge)-donor or acceptor-(π conjugated bridge)-donor-(π conjugated bridge)-acceptor structures were studied by density functional theory. Studies show that different combinations of the donor, acceptor, heterocycle, $-C\equiv C-$ and $-N=N-$ moieties, and orientation of heterocycle remarkably affect the second-order NLO responses. The complexes containing electronic acceptor matched with the direction of charge transfer possess remarkable large molecular second-order polarizabilities. Electronic transitions to crucial excited states show that x-polarized transition, contributed to the off-diagonal second-order polarizability tensor (β_{zx}), possesses

lower excited energy compared with z-polarized transition which accounted for the diagonal second-order polarizability tensor (β_{zz}) and thus led to the large in-plane nonlinear anisotropy ($u = \beta_{zx}/\beta_{zz}$) value, as well as good two-dimensional (2-D) second-order NLO properties. These complexes can be used as excellent 2-D second-order NLO materials from the standpoint of both large β and u values.

Keywords Organoimido · Hexamolybdates · Charge transfer · Electronic transition · Nonlinear optical property

1 Introduction

The design and synthesis of second-order nonlinear optical (NLO) materials have been receiving more and more attention due to their potential applications in optoelectronic technology [1–3]. On the basis of the experimental and theoretical explorations, several principles to enhance second-order NLO responses have been proposed, such as planar donor- π conjugated bridge-acceptor (D- π -A) model [4], bond length alternation (BLA) theory [5], auxiliary donors and acceptors model of heterocycle [6–8], and twisted π -electron system etc. [9–11]. Directed by these strategies, the large second-order NLO responses can be achieved by optimizing the D/A strengths and/or extending the conjugated bridge [12].

In the past two decades, considerable efforts have been focused on the development of one-dimensional (1-D) NLO materials. However, there are several apparent problems for the 1-D NLO molecules to construct the large bulk NLO materials, such as the dipole–dipole interaction [13]. The 1-D push–pull molecules always possess large permanent dipole moment, which would favor the

Electronic supplementary material The online version of this article (doi:10.1007/s00214-008-0501-0) contains supplementary material, which is available to authorized users.

Y. L. Si · C. G. Liu · E. B. Wang (✉) · Z. M. Su (✉)
Key Laboratory of Polyoxometalate Science
of Ministry of Education, Faculty of Chemistry,
Northeast Normal University, 130024 Changchun,
People's Republic of China
e-mail: wangeb889@nenu.edu.cn

Z. M. Su
e-mail: zmsu@nenu.edu.cn

Y. L. Si
College of Resource and Environmental Science,
Jilin Agricultural University, 130118, Changchun, Jilin,
People's Republic of China

formation of the centrosymmetric arrangement in the crystal. Thus, no bulk NLO responses were observed in the 1-D push–pull molecules. Another problem arises from the phase-matching orientations of 1-D molecules in the crystal [14]. For example, the typical PNA molecule, the 1, 2, m, and mm2 crystal point groups are in better agreement with the optical phase-matching conditions, the angle between the molecular charge transfer (CT) axis and the crystal principal dielectric axis is predicted as 54.7° (or 125.3°). As a result, only one β tensor component is assumed to be nonnegligible. It is well known that the macroscopic NLO polarizabilities equal the summation of individual molecules. Obviously, the phase-matching orientations of 1-D compounds are allowed to recover fewer macroscopic NLO responses in crystal materials. Recently, Würthner group [15, 16] and Koleva group [17–20] synthesised and characterized a series of 1-D organic compounds exhibiting excellent NLO response due to strong self-aggregation.

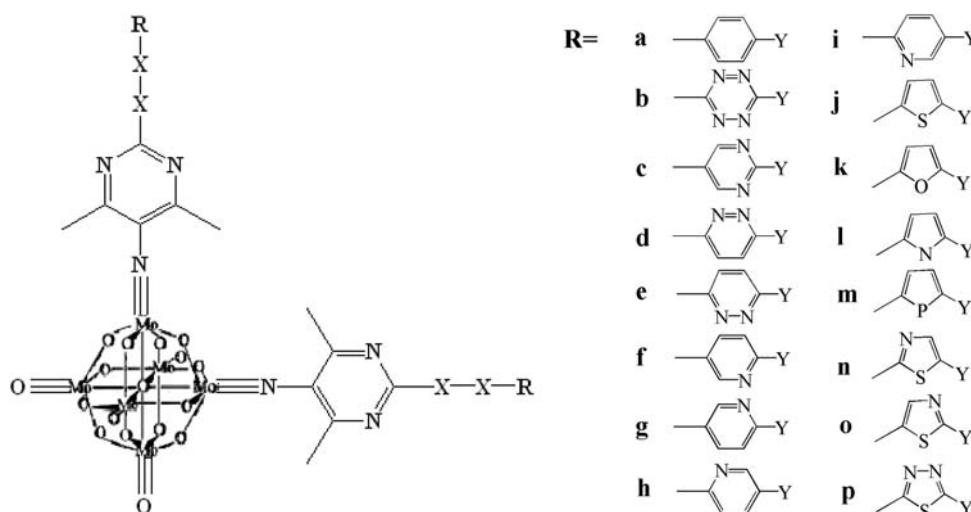
Thus, the multidimensional compounds with large off-diagonal β tensor components are highly desirable to probe by using experimental and theoretical methods. Studies show that various organic multidimensional compounds can be used as excellent candidates for the second-order NLO applications [21–27]. These compounds have exhibited the following merits compared with the 1-D compounds, (1) the multidimensional NLO compounds display large off-diagonal β tensor components because of the high oscillator strength, low-lying energy excited states with electron transition dipole moment between two states perpendicular to the dipolar axis, and (2) the multidimensional NLO molecules show an increased stability of polar order in poled polymers and Langmuir–Blodgett (LB) films, and (3) comparing with the 1-D structures, the multidimensional NLO compounds can increase second-order NLO responses without losses of transparency in the visible region, which may offer advantage of better nonlinearity/transparency tradeoff, and (4) the multidimensional NLO compounds under the phase-matching orientations can offer larger macroscopic NLO responses because of large off-diagonal β tensor component compared with the 1-D compounds. However, few examples of the systematic optimization and determination of off-diagonal β tensor component have been reported in literatures. Most of them reported in literatures are based on the benzene derivatives [24], ruthenium (II) or iron (II) complexes [28–30], and dipolar D-A-substituted Schiff base complexes [2, 27]. Recently, the investigation of 2-D carbazole-cored chromophores demonstrated that introduction of heterocycles auxiliary donor can significantly enhance the off-diagonal β tensor component because of the strong, low-lying energy, perpendicular CT transition [31]. Furthermore, Würthner group [32, 33] and Koleva group [34] characterized three kinds of 2-D organic

compounds, which could become potential NLO materials due to the strong noncovalent interactions.

Polyoxometalates (POMs) are a rich class of inorganic cluster systems and exhibit remarkable chemical and physical properties, which have been applied to a variety of fields, such as medicine, catalysis, biology, analytical chemistry, and materials science [35]. Among different types of POMs, organically derived POMs have been extensively studied, especially; charge-transfer covalently bonded organoimido derived hexamolybdate clusters have attracted particular interest because the organic π electrons can extend their conjugation to the inorganic framework, which would generate the strong d- π interactions [36–39]. A series of organoimido derivatives containing various delocalized π -organic ligands have been synthesized [37], and the efficient CT between the organic ligands and hexamolybdate clusters has been reported according to the electronic spectroscopic studies, which demonstrates that the Mo–N π bond of organoimido derived hexamolybdate cluster is delocalized on the organic conjugated π system. In general, an excellent charge transfer is the premise of larger NLO response. Recently, our group has been interested in the investigations on the NLO properties of organoimido derivatives of hexamolybdates, which exhibit remarkable large second or third-order NLO response. The CT from organoimido to polyanion is responsible for the NLO response [40–42].

The substitution of the terminal oxygen of hexamolybdate clusters with organoimido ligands provides the effective approach to synthesize difunctionalized hexamolybdates possessing the C_{2v} symmetry [37], which can be utilized to build 2-D \wedge -shaped structures. On the other hand, introduction of various heteroatoms in the conjugated polymer is a well-known approach to change their electronic and optical properties, increase chemical stabilities and introduce flexibilities for further molecular engineering [6–8, 43]. Moreover, aromatic heterocycles can modulate the NLO responses through the different aromatic delocalization energy, the different charge density, the various orientation of the heterocycles dipole moment, even the variable longitudinal charge-transfer interaction due to the auxiliary electron donor/acceptor nature of the heterocycles. All of these factors can be properly chosen to design the good NLO materials. For the organoimido derivatives of hexamolybdates, how to tune these factors to obtain the cooperativity of charge-transfer between organoimido and hexamolybdate, and enhance the second-order NLO response is not fully studied. Thus, we designed two kinds of complexes (four series of complexes are shown in Fig. 1), donor-(π conjugated bridge)-acceptor-(π conjugated bridge)-donor (DAD) (set I and II) and acceptor-(π conjugated bridge)-donor-(π conjugated bridge)-acceptor (ADA) (set III and IV), to probe donor and acceptor

Fig. 1 Structural formulas for all complexes (Set I: X = C, Y = NH₂, Set II: X = N, Y = NH₂, Set III: X = C, Y = NO₂, Set IV: X = N, Y = NO₂)



substituted, different conjugated bridges, and various heterocycles effects on second-order NLO responses. The four complexes were chosen as the reference systems (Ia in set I, IIa in set II, IIIa in set III, and IVa in set IV).

2 Computational details

All calculations were performed by using Amsterdam Density Functional (ADF) program developed by daerends et al. [44–46], and the local exchange correlation approximation of Vosko, Wilk, and Nusair was used along with the correction of Becke and Perdew [47, 48]. Triple- ζ basis set of Slater orbitals (STO) augmented with a set of polarization functions was used to describe the valence electrons of main group atoms and the metal atoms. The 1s shell of C, N, O, 1s to 2p shells for S, P, and 1s to 3d shells for Mo have been treated by the frozen core approximation, and described by means of single Slater functions. The relativistic effects were taken into account by using the zero-order regular approximation (ZORA) [49–52]. The van Leeuwen–Baerends XC potential (LB94) was chosen for calculations of all the response properties [53]. The adiabatic local density approximation (ALDA) was applied for the evaluation of the first and second functional derivatives of the XC potential. The transition energies and transition moments can be obtained from the calculated results on the basis of the TD model of ADF. The

integration parameter used to determine the precision of the numerical integral, was set to 6.0. The default optimization convergence criteria were used in the ADF.

3 Results and discussion

3.1 The choice of studied models

To generate 2-D NLO properties, the two organic ligands were introduced with an angle of $\sim 90^\circ$ relative to each other. Why the pyrimidine ring is chosen to attach to the Mo–N bond as the first organic π conjugated bridge? Our previous studies have shown that replacement of a carbon atom with a nitrogen atom within the conjugated substituent can remarkably increase the second-order NLO response, which is attributed to a larger amount of electronegativity in the nitrogen atom than that in the carbon atom [54]. Firstly, we design three simple complexes to test this effect on POMs (Fig. 2). The calculated static second-order polarizabilities, second-harmonic generation (SHG), optical rectification (OR), and electron-optic Pockels effect (EOPE) values [55–59] at the optical frequency ($\hbar\omega = 0.65$ eV) are presented in Table 1. We find that the replacement of the benzene ring with the heteroaromatic ring containing two nitrogen atoms significantly enhances the second-order NLO responses not only static but also dynamic values. Thus, the pyrimidine ring is chosen to

Fig. 2 Calculated models of three simple complexes

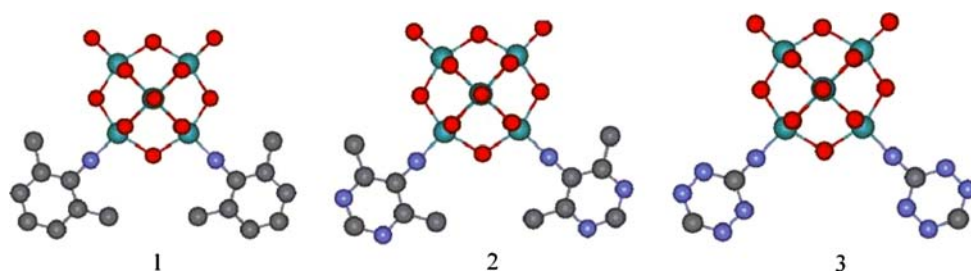


Table 1 The calculated second-order polarizability ($\times 10^{-30}$ cm⁵ esu⁻¹) at $\hbar\omega = 0.0$ eV (static) and $\hbar\omega = 0.65$ eV (SHG, EOPE, and OR) for simple systems 1–3

	Static	SHG	EOPE	OR
1	-697.50	-1,009.90	794.45	-786.55
2	-942.02	-1,141.00	1,007.60	-1,001.00
3	-689.80	-1,073.90	791.20	-791.96

attach to the Mo–N bond. Subsequently, to obtain the cooperativity of charge-transfer between organoimido and hexamolybdate, and enhance the second-order NLO response, $-\text{C}\equiv\text{C}-$ moiety, $-\text{N}=\text{N}-$ moiety, various five- and six-membered rings, donor (NH_2), and acceptor (NO_2) are attached to the pyrimidine ring, respectively. Then, four kinds of studied complexes (I–IV) are formed. Among them, DAD complexes are in set I and II, ADA complexes are in set III and IV.

3.2 DAD-like complexes (set I and II)

3.2.1 The static second-order NLO properties

In set I, the organic π conjugated bridges are comprised of two aromatic rings separated by an ethyne moiety (Ia–Ip). Set II is the substitution of the $-\text{C}\equiv\text{C}-$ moiety in set I with $-\text{N}=\text{N}-$ moiety. The calculated values of the second-order polarizabilities and their tensor components are listed in Table 2. According to the results, we can find the following results: (1) in general, the NLO values of the complexes containing $-\text{C}\equiv\text{C}-$ moiety are larger than those containing $-\text{N}=\text{N}-$ moiety. (2) Some five-membered rings derivatives display larger second-order polarizabilities than their benzenoid analogues (Ij, Im, In, Io, Ip vs. Ia). (3) The second-order polarizabilities of six-membered rings derivatives are not only larger than that of the benzenoid analogues, but also larger than that of the five-membered rings derivatives. (4) As expected, complex Ib containing tetrazine rings generates the largest second-order polarizability in set I. However, the second-order polarizability magnitude of different regiochemistries, such as, pyrimidine (Ic), pyridazine (Id, Ie), and pyridine (If, Ig, Ih, Ii) is different. Replacement of phenyl ring with pyridine ring generates four different complexes (If, Ig, Ih, Ii). Complexes Ih and Ii with heteroatom adjacent to ethyne moiety yield only a smaller increase in the second-order polarizabilities compared with the reference complex Ia, and the orientation of the pyridine within the complex have no substantial effect. By contrast, complexes If and Ig with heteroatom adjacent amido afford a larger increase in the second-order polarizabilities, and the relative orientation of the pyridine ring within the complex does not play a crucial role in

Table 2 The calculated second-order polarizabilities ($\beta_{\text{vec}} \times 10^{-30}$ cm⁵ esu⁻¹), tensor (β_{zzz} and β_{zxx}), anisotropy ($u = \beta_{\text{zxx}}/\beta_{\text{zzz}}$), excitation energy (ΔE_{ge} , eV), and oscillator strength (f_{oc} , a.u.) in DAD-like complexes (set I and II)

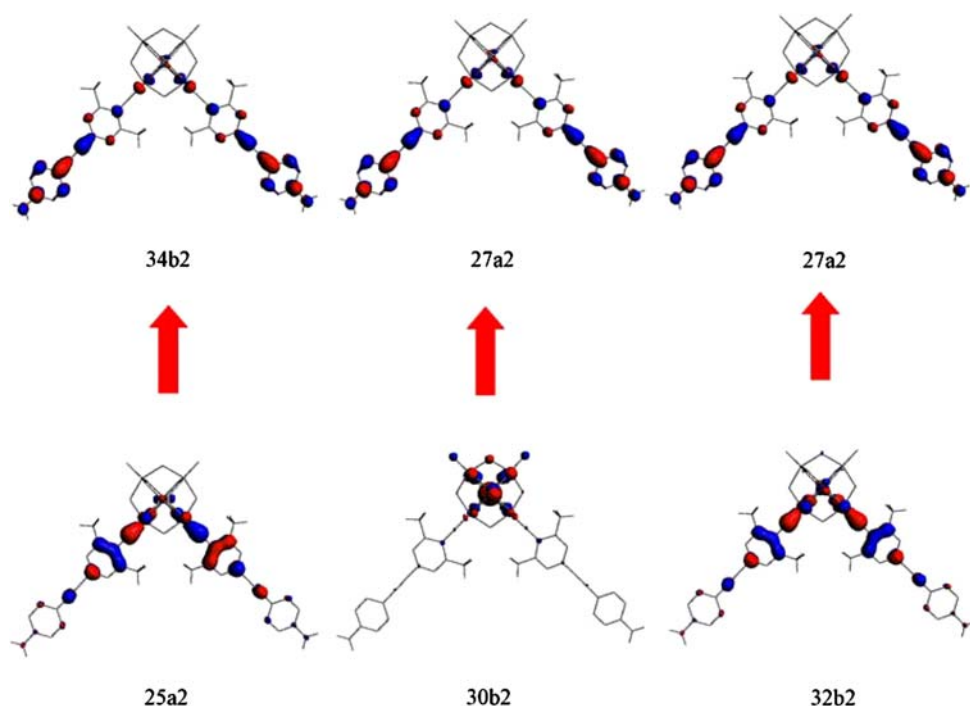
Complex	β_{zzz}	β_{zxx}	u	β_{vec}	ΔE_{ge}	f_{oc}
Set I						
Ia	45.03	62.22	1.38	-64.94	2.29	1.11
Ib	218.75	369.92	1.69	-353.90	1.97	0.60
Ic	158.15	261.82	1.66	-252.76	2.13	1.04
Id	169.56	261.24	1.54	-259.27	2.21	0.54
Ie	147.82	259.90	1.76	-245.16	2.22	0.56
If	116.55	177.16	1.52	-176.98	2.15	0.77
Ig	108.15	179.19	1.66	-172.98	2.15	0.70
Ih	91.50	123.53	1.35	-129.67	2.29	0.59
Ii	76.45	133.86	1.75	-126.66	2.22	0.66
Ij	65.33	105.28	1.61	-103.10	2.32	1.12
Ik	-8.92	7.87	0.88	0.14	2.42	1.27
Il	-47.81	-62.59	1.31	65.73	2.43	0.76
Im	56.62	72.38	1.28	-78.73	2.37	0.99
In	112.56	168.21	1.49	-169.35	2.27	1.02
Io	117.03	168.54	1.44	-172.09	2.29	1.08
Ip	158.27	224.35	1.42	-230.46	2.21	1.04
Set II						
IIa	38.75	97.29	2.51	-82.53	1.96	0.84
IIb	77.41	191.18	2.47	-161.97	2.05	1.51
IIc	57.07	143.59	2.52	-121.15	2.07	1.06
IId	57.02	127.51	2.24	-111.68	2.10	1.25
IIe	55.49	171.13	3.08	-136.61	2.02	0.80
IIf	38.26	114.59	3.00	-92.47	2.11	0.98
IIg	73.03	187.66	2.57	-157.49	1.95	1.32
IIh	57.03	135.74	2.38	-116.83	1.90	1.14
IIi	76.92	185.99	2.42	-158.75	1.96	1.11
IIj	52.85	121.18	2.29	-105.45	2.13	1.19

determining the second-order polarizability. According to DFT calculations, introduction of heterocycles in set II also enhances the second-order NLO properties compared with the reference complex IIa. The complex IIb (tetrazine ring) displays the largest second-order NLO response in set II. The regiochemistry of pyridazine and thiazole rings (IId and IIe, IIg and IIi) also affects their nonlinear properties in set II. However, the influence of heterocycles on the second-order polarizability in set II is smaller than that in set I. So, only partial complexes containing heterocycles are studied in set II.

3.2.2 The character of electronic transition

From Table 2, the significant enhancement of the off-diagonal components β_{zxx} in those complexes is observed. The off-diagonal components of most of complexes Ia–Ip

Fig. 3 Molecular orbitals associated to the crucial excited state of complex Ib



that Mo–N bonds are related to the intense, and low-lying energy CT transitions, however the Mo–O bonds in hexamolybdate do not take part in this LMCT process, which demonstrates that extents of organic π electron delocalization in the hexamolybdate cluster are on the two Mo–N bonds. Our calculations also give the same results (see orbitals 25a2, 32b2). The electronic density is mainly located on Mo–N bond and adjacent pyrimidine ring in 25a2 and 32b2 orbitals, and there is no electron density on other segments of hexamolybdate. Secondly, the hexamolybdate cluster in set I and II acts as rather the electron donor than the electron acceptor. It is well known that POMs anions can be reduced by addition of a number of electrons in reduction processes, and thus display the feature of electron acceptor. However, introduction of organic ligands into hexamolybdates results in the formation of the complexes which bears many similarities to metal complexes with organic π conjugated ligands. For example, the crucial absorptions of complex Ib are due to 25a2 \rightarrow 34b2, 32b2 \rightarrow 27a2, and 30b2 \rightarrow 27a2 transitions, and can be assigned as CT from hexamolybdate cluster and adjacent pyrimidine ring to the ethyne moiety and tetrazine rings. The organic ligand fragment is the CT axis, while Mo–N bond and hexamolybdate cluster act as an electron donor. It should be noted that the organometallic substituted, $[\text{SiW}_9\text{O}_{37}(\text{SnPh})_3]^{7-}$, also displays the same feature [61]. Thus, the DAD-like structure in these complexes might not be favored to generate the large second-order NLO responses because the unsuitable introduction of amido electron donor generate the reverse D–A substitutions corresponding to the direction of CT.

3.3 ADA-like complexes (set III and IV)

The calculated values of the second-order polarizabilities and their tensor components are listed in Table 4 for set III and IV. In general, the β values in set III and IV are great larger than those of set I and II. For example, the static second-order polarizability of reference complex IIIa is ~ 14 times larger than that of the reference complex Ia. Compared with the two complexes structures, the enhancement of β value is mainly caused by the acceptor substituted effects. Compared with between III and IV, the NLO values of the complexes containing $-\text{C}\equiv\text{C}-$ moiety are also larger than those of $-\text{N}=\text{N}-$ moiety. To our studied complexes, the $-\text{C}\equiv\text{C}-$ conjugated bridge is better than $-\text{N}=\text{N}-$ conjugated bridge. The orbitals associated with the crucial excited states of the complex IIIb are shown in Fig. 4. It can be seen that the crucial excited state transition is mainly formed by the contributions of 26a2 \rightarrow 34b2, 31b2 \rightarrow 27a2, and 33b2 \rightarrow 27a2 transitions. Clearly, these excitations mostly consist of CT from the M–N bond and the hexamolybdate cluster to the tetrazine ring and nitril acceptor. Thus, ADA-like complexes in set III provide the matched structures corresponding to the direction of the CT. These advantages on the CT of complexes in set III are also reflected on the lower transition energy of crucial excited states compared to the relevant complex in set I (see Tables 2, 4). For example, the first transition energy of crucial excited states in complex Ia is ~ 1.60 times larger than that of complex IIIa. The low-lying transition energy and large extent of CT would enhance the second-order NLO

Table 4 The calculated second-order polarizabilities ($\beta_{\text{vec}} \times 10^{-30}$ cm⁵ esu⁻¹), tensor (β_{zzz} , β_{zxx}), anisotropy ($u = \beta_{\text{zxx}}/\beta_{\text{zzz}}$), excitation energy (ΔE_{ge} , eV), and oscillator strength (f_{oc} , a.u.) in ADA-like Complexes (set III and IV)

Complex	β_{zzz}	β_{zxx}	u	β_{vec}	ΔE_{ge}	f_{oc}
Set III						
IIIa	480.05	977.34	2.04	875.68	1.44	0.56
IIIb	326.69	666.50	2.04	596.94	1.46	1.11
IIIc	480.01	960.38	2.00	865.31	1.43	0.68
III d	427.19	864.00	2.02	-776.08	1.36	0.58
IIIe	423.16	880.40	2.08	-783.22	1.37	0.62
III f	478.74	979.92	2.05	-876.28	1.42	0.59
III g	488.37	976.58	2.00	-880.26	1.42	0.59
III h	416.73	854.58	2.05	-764.11	1.43	0.75
III i	411.86	856.57	2.08	-762.21	1.43	0.75
III j	462.51	718.31	1.55	-709.50	1.52	0.50
III k	414.55	650.00	1.57	-639.45	1.56	0.50
III l	464.81	701.30	1.51	-700.31	2.36	0.46
III m	581.82	844.45	1.45	-857.32	1.29	0.47
III n	443.99	683.31	1.54	-677.49	2.25	0.56
III o	456.26	688.56	1.51	-664.60	1.42	0.51
III p	468.74	691.44	1.48	-697.28	2.18	1.57
Set IV						
IVa	240.94	706.28	2.93	-569.46	1.55	0.84
IVb	178.77	502.03	2.81	-409.26	1.62	1.43
IVc	249.99	696.75	2.79	-568.93	1.59	0.93
IVd	249.92	696.47	2.79	-568.97	1.50	0.80
IVe	236.41	695.77	2.94	-560.39	1.48	0.75
IVf	247.00	713.04	2.89	-576.83	1.57	0.69
IVg	246.38	690.96	2.80	-563.55	1.56	0.90
IVh	216.56	635.08	2.93	-512.21	1.55	1.06
IVi	208.26	618.25	2.97	-496.94	1.54	1.03
IVj	168.38	338.63	2.01	-305.11	1.65	1.23
IVk	144.75	262.38	1.81	-244.73	1.71	1.23
IVl	154.73	284.19	1.84	-263.83	1.72	0.97
IVm	209.09	395.92	1.89	-364.32	2.13	0.71
IVn	160.62	299.26	1.86	-276.78	1.65	1.09
IVo	194.17	353.05	1.82	-329.20	1.59	1.02
IVp	233.61	402.85	1.72	-382.79	1.53	0.54

responses, which is well agreement with our DFT calculated results (see Tables 2, 4).

Compared with the reference complex IIIa, introduction of the heterocycle can not effectively enhance the second-order NLO responses in set III. For example, the β value of complex IIIg containing pyridine ring is only slightly larger than that of IIIa. However, the relative orientation of the pyridine ring within the complex plays a crucial role in determining the NLO response. For complexes IIIf and IIIg, the heteroatom N is close to acceptor and displays the larger β value in set III. Thus, the static second-order

polarizability for the pyridine derivatives increases in the order IIIi < IIIh < IIIf < IIIg. In four sets (set I–IV), the second-order polarizabilities of same orientation (heteroatom N is closed to the donor/acceptor) of the pyridine ring are larger than that of other pyridine analogues. The increase on second-order polarizability can be rationalized by the dipole moment direction of the pyridine. In complexes If, Ig, IIf, IIg, IIIf, IIIg, IVf, and IVg, the dipole moment of the pyridine ring displays approximately parallel to the direction of the dipole moment of the complex (see Fig. 5), as well as the large second-order NLO properties. This feature is agreement with the “matched” structure of the thiazole ring in thiazole and thiophene analogues of D-A stilbenes, and the second-order polarizability increases when the dipole moment of the thiazole ring reinforces the molecular dipole [6].

In set IV, introduction of the heterocycles can not enhance the second-order NLO responses effectively compared with the reference complex IVa. Although, the complex IVf displays the largest static second-order NLO responses in set IV, the β value of complex IVf is only slightly larger than that of complex IVa. On the other hand, comparing with set III, introduction of –N=N– can not increase the β values, but the in-plane nonlinear anisotropy value yields a enhancement in set IV because the angle between two D-A segments increases to $\sim 100^\circ$.

3.4 Comparison between DAD-like and ADA-like complexes

On the basis of the large second-order NLO responses of set I and set III, we take reference complexes Ia and IIIa as the examples to analyze the 2-D second-order NLO responses. The crucial excited states, which significantly contribute to the second-order polarizabilities, are shown in Table 5. It can be found that the crucial absorption of complex Ia is assigned as metal-to-ligand (ML) CT and cluster to ligand CT transitions (see Table S1). For complex IIIa, the crucial absorptions are assigned to MLCT, cluster to ligand CT, and ILCT transitions (see Table S3). It suggests that the second-order NLO properties of complexes Ia, IIIa are related to the Mo–N bond and organic ligands, while introduction of the electronic donor and acceptor has no influence on the CT direction. But, our calculations predict that these absorption bands bathochromically shift (lower transition energies) as introduction of electronic acceptor compared with that of electronic donor. The lower transition excited energies can lead to larger second-order NLO response, which is in agreement with our calculated results.

The intense and low-lying energy CT transition of complex Ia is the x-polarized transition (B_1 symmetry). By contrast, the crucial absorptions of complex IIIa are the x-polarized transition (B_1 symmetry) and z-polarized

Fig. 4 Molecular orbitals associated to the crucial excited state of complex IIIb

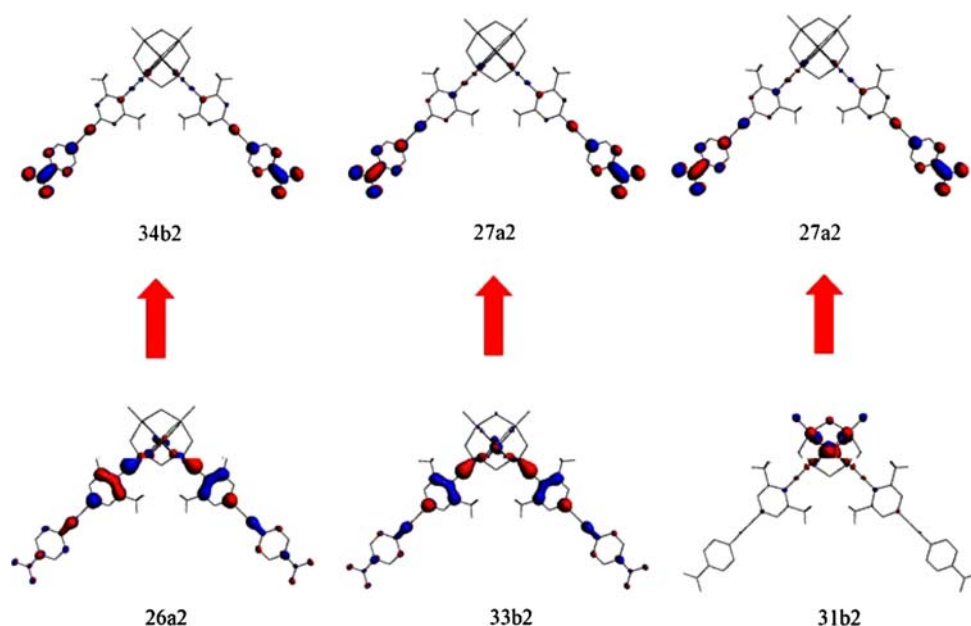


Fig. 5 Dipole moment of pyridine ring and complexes IIIi and IIIg

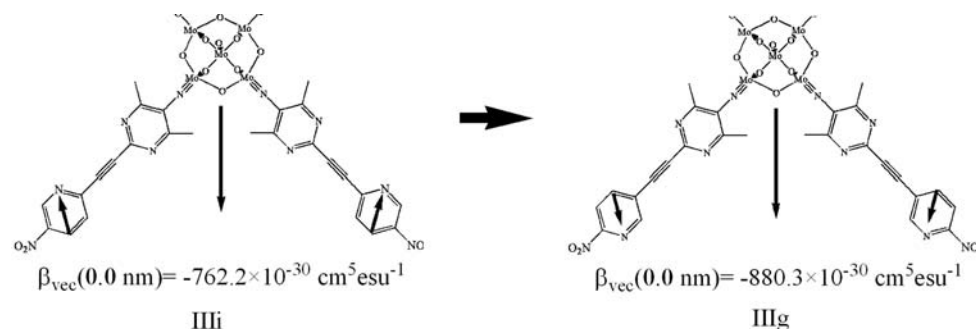


Table 5 Computed linear optical parameters and static second-order polarizabilities ($\times 10^{-30} \text{ cm}^5 \text{ esu}^{-1}$) for complexes Ia and IIIa

Complex	E_{ge} (eV) (λ nm)	f_{oc}	Symmetry (polarization)	β_{zzz}	β_{zxx}	β_{vec}	u
Ia	2.29 (541.4)	1.11	B1 (X)	45.03	62.22	64.9	1.38
IIIa	1.44 (861.0)	0.56	B1 (X)	480.05	977.34	875.7	2.04
	2.33 (532.1)	0.53	B1 (X)				
	1.51 (821.1)	0.51	A1 (Z)				

transition (A_1 symmetry), respectively (see Table 5). As mentioned above, the z-polarized transition contributes to the diagonal second-order polarizability tensor term, and x-polarized transition accounts for the off-diagonal second-order polarizability tensor term. Comparing with Ia, intense absorption bands associated with the x-polarized transition are red shifted by about 320 nm in complex IIIa due to introduction of electronic acceptor. The lower transition energies would enhance the second-order NLO responses, thus, the off-diagonal second-order polarizability tensor β_{zxx} of IIIa is 15.7 times larger than that of complex Ia. For complex IIIa, the low-lying energy CT excited states associated with the z-polarized transition also enhance the diagonal second-order polarizability tensor, so the β_{zzz}

value of complex IIIa is 10.7 times larger than that of complex Ia. Obviously, the enhancement of diagonal second-order polarizability tensor (β_{zzz}) is weaker than that of off-diagonal second-order polarizability tensor (β_{zxx}) in complex IIIa. Thus, the in-plane nonlinear anisotropy ($u = \beta_{zxx}/\beta_{zzz}$) value increases to 2.04, and complex IIIa displays a good 2-D second-order NLO property.

4 Conclusion

In the present paper, we have studied electronic structures and the 2-D second-order NLO properties of a series of charge-transfer covalently bonded organoimido derived

hexamolybdate cluster and elucidated structure-property relationships from the micromechanism by using DFT calculations. The results show that (1) introduction of electronic acceptor can remarkably enhance second-order NLO responses because the cooperativity of charge-transfer between organoimido and hexamolybdate are matched; (2) the second-order polarizabilities of complexes containing $-C\equiv C-$ moiety are larger than those of complexes containing $-N=N-$ moiety; (3) these complexes can become excellent 2-D NLO candidates because x-polarized transition contributes to the off-diagonal second-order polarizability tensor (β_{zxx}) according to electronic transitions to crucial excited states; (4) complexes containing $-N=N-$ moiety exhibit larger in-plane nonlinear anisotropy ($u = \beta_{zxx}/\beta_{zzz}$) value compared with complexes containing $-C\equiv C-$ moiety, because x-polarized transition possesses lower excited energy compared with the energy of z-polarized transition; (5) the second-order NLO properties of studied complexes are sensitive to the orientation of the heterocycles because of dipole moment direction in different heterocycles. In summary, the cooperativity of CT between organoimido and hexamolybdate is matched in set III which can be used as excellent 2-D second-order NLO candidates from the standpoint of both large β and u values.

Acknowledgments We gratefully acknowledge the financial support from the National Natural Science Foundation of China (Project Nos. 20701005, 20701006, 20373009 and 20703008), Chang Jiang Scholars Program (2006), Program for Changjiang Scholars and Innovative Research Team in University (IRT0714), the National High-tech Research and Development Program (863 Program 2007AA03Z354).

References

- Kanis DR, Ratner MA, Marks TJ (1994) *Chem Rev* 94:195. doi:10.1021/cr00025a007
- Di Bella S (2001) *Chem Soc Rev* 30:355. doi:10.1039/b100820j
- Lacroix PG (2001) *Eur J Inorg Chem* 339. doi:10.1002/1099-0682(200102)2001:2<339::AID-EJIC339>3.0.CO;2-Z
- Zyss J, Ledoux I (1994) *Chem Rev* 94:77. doi:10.1021/cr00025a003
- Meyers F, Marder SR, Pierce BM, Bredas JL (1994) *J Am Chem Soc* 116:10703. doi:10.1021/ja00102a040
- Breitung EM, Shu CF, McMahon RJ (2000) *J Am Chem Soc* 122:1154. doi:10.1021/ja9930364
- Rao Varanasi P, Jen AK-J, Chandrasekhar J, Namboothiri INN, Rathna A (1996) *J Am Chem Soc* 118:12443. doi:10.1021/ja960136q
- Albert ID, Marks TJ, Ratner MA (1997) *J Am Chem Soc* 119:6575. doi:10.1021/ja962968u
- Kang H, Facchetti A, Jiang H, Cariati E, Righetto S, Ugo R, Zuccaccia C, Macchioni A, Stern CL, Liu Z, Ho ST, Brown EC, Ratner MA, Marks TJ (2007) *J Am Chem Soc* 129:3267. doi:10.1021/ja0674690
- Kang H, Facchetti A, Zhu P, Jiang H, Yang Y, Cariati E, Righetto S, Ugo R, Zuccaccia C, Macchioni A, Stern CL, Liu Z, Ho ST, Marks TJ (2005) *Angew Chem Int Ed Engl* 44:7922. doi:10.1002/anie.200501581
- Yang JS, Liao KL, Li CY, Chen MY (2007) *J Am Chem Soc* 129:13183. doi:10.1021/ja0741022
- Shi YQ, Zhang C, Zhang H, Bechtel JH, Dalton LR, Robinson BH, Steier WH (2000) *Science* 288:119
- Liao Y, Bhattacharjee S, Firestone KA, Eichinger BE, Paranj R, Anderson CA, Robinson BH, Reid PJ, Dalton LR (2006) *J Am Chem Soc* 128:6847. doi:10.1021/ja057903i
- Yang M, Champagne B (2003) *J Phys Chem A* 107:3942. doi:10.1021/jp0272567
- Würthner F, Yao S, Heise B, Tschierske C (2001) *Chem Commun (Camb)* 2260. doi:10.1039/b106413d
- Rusch U, Yao S, Wortmann R, Würthner F (2006) *Angew Chem* 118:7184. doi:10.1002/ange.200602286
- Kolev T, Koleva BB, Spitteller M, Mayer-Figge H, Sheldrick WS (2008) *Dyes Pigments* 79(1):7. doi:10.1016/j.dyepig.2007.12.007
- Kolev T, Koleva BB, Stoyanov S, Spitteller M, Petkov I (2008) *Spectrochim Acta Part A* 70(5):1087. doi:10.1016/j.saa.2007.10.017
- Koleva BB, Kolev T, Seidel RW, Mayer-Figge H, Spitteller M, Sheldrick WS (2008) *J Phys Chem A* 112:2899. doi:10.1021/jp710765v
- Kolev T, Koleva BB, Spitteller M, Sheldrick WS, Mayer-Figge H (2007) *J Phys Chem A* 111:10084. doi:10.1021/jp068761x
- Zyss J (1993) *J Chem Phys* 98:6583. doi:10.1063/1.464802
- Moylan CR, Ermer S, Lovejoy SM, McComb I-H, Leung DS, Wortmann R, Krdmer P, Twieg RJ (1996) *J Am Chem Soc* 118:12950. doi:10.1021/ja962673g
- Wortmann R, Glania C, Kramer P, Matschiner R, Wolff JJ, Kraft S, Treptow B, Barbu E, Langle D, Gorlitz G (1997) *Chem Eur J* 3:1765. doi:10.1002/chem.19970031107
- Wolff JJ, Langle D, Hillenbrand D, Wortmann R, Matschiner R, Glania C, Kramer P (1997) *Adv Mater* 9:138. doi:10.1002/adma.19970090209
- Tomonari M, Ookubo N, Takada T (1997) *Chem Phys Lett* 266:488. doi:10.1016/S0009-2614(97)00054-7
- Liu YJ, Liu Y, Zhang DJ, Hu HQ, Liu CB (2001) *J Mol Struct* 570:43. doi:10.1016/S0022-2860(01)00479-3
- Di Bella S, Fargala I, Ledoux I, Zyss J (2001) *Chem Eur J* 7:3738. doi:10.1002/1521-3765(20010903)7:17<3738::AID-CHEM3738>3.0.CO;2-I
- Coe BJ, Harris JA, Jones LA, Brunshwing BS, Song K, Clays K, Garin J, Orduna J, Coles SJ, Hursthouse MB (2005) *J Am Chem Soc* 127:4845. doi:10.1021/ja0424124
- Coe BJ (2006) *Acc Chem Res* 39:383. doi:10.1021/ar050225k
- Coe BJ, Harris JA, Brunshwing BS, Asselberghs I, Clays K, Garin J, Orduna J (2005) *J Am Chem Soc* 127:13399. doi:10.1021/ja053879x
- Liu CG, Qiu YQ, Su ZM, Yang GC, Sun SL (2008) *J Phys Chem C* 112:7021. doi:10.1021/jp0762673
- Lohr A, Lysetska M, Würthner F (2005) *Angew Chem Int Ed Engl* 44:5071. doi:10.1002/anie.200500640
- Würthner F, Yao S, Beginn U (2003) *Angew Chem Int Ed Engl* 42:3247. doi:10.1002/anie.200351414
- Koleva BB, Stoyanov S, Kolev T, Petkov I, Spitteller M (2008) *Spectrochim Acta Part A* 71:847. doi:10.1016/j.saa.2008.02.036
- Hill CL, White GC (1998) *Chem Rev* 98:1. doi:10.1021/cr960395y
- Stark JL, Young VG Jr, Maatta EA (1995) *Angew Chem Int Ed Engl* 34:2547
- Peng ZH (2004) *Angew Chem Int Ed Engl* 43:930. doi:10.1002/anie.200301682

38. Xu BB, Peng ZH, Wei YG, Powell DR (2003) *Chem Commun (Camb)* 2562. doi:[10.1039/b307415c](https://doi.org/10.1039/b307415c)
39. Xu BB, Lu M, Kang JH, Wang DG, Brown J, Peng ZH (2005) *Chem Mater* 17:2841. doi:[10.1021/cm050188r](https://doi.org/10.1021/cm050188r)
40. Yan LK, Yang GC, Guan W, Su ZM, Wang RS (2005) *J Phys Chem B* 109:22332. doi:[10.1021/jp0542120](https://doi.org/10.1021/jp0542120)
41. Yang GC, Guan W, Yan LK, Su ZM, Xu L, Wang EB (2006) *J Phys Chem B* 110:23092. doi:[10.1021/jp062820p](https://doi.org/10.1021/jp062820p)
42. Yan LK, Jin MS, Zhuang J, Liu CG, Su ZM, Sun CC (2008) *J Phys Chem A* 112:9919. doi:[10.1021/jp804342h](https://doi.org/10.1021/jp804342h)
43. Nandi PK, Panja N, Ghanty TK (2008) *J Phys Chem A* 112:4844. doi:[10.1021/jp710010f](https://doi.org/10.1021/jp710010f)
44. Te Velde G, Bickelhaupt FM, Baerends EJ, Fonseca Guerra C, van Gisbergen SJA, Snijders JG, Ziegler T (2001) *J Comput Chem* 22:931. doi:[10.1002/jcc.1056](https://doi.org/10.1002/jcc.1056)
45. Fonseca Guerra C, Snijders JG, Te Velde G, Baerends EJ (1998) *Theor Chem Acc* 99:391
46. ADF2006 01, SCM Theoretical Chemistry, Vrije Universiteit, Amsterdam, The Netherlands, <http://www.scm.com>
47. Becke AD (1988) *Phys Rev A* 38:3098. doi:[10.1103/PhysRevA.38.3098](https://doi.org/10.1103/PhysRevA.38.3098)
48. Perdew JP (1986) *Phys Rev B* 33:8822. doi:[10.1103/PhysRevB.33.8822](https://doi.org/10.1103/PhysRevB.33.8822)
49. Chang C, Pelissier M, Durand M (1986) *Phys Scr* 34:394. doi:[10.1088/0031-8949/34/5/007](https://doi.org/10.1088/0031-8949/34/5/007)
50. van Lenthe E, Baerends EJ, Snijders JG (1993) *J Chem Phys* 99:4597. doi:[10.1063/1.466059](https://doi.org/10.1063/1.466059)
51. van Lenthe E, Baerends EJ, Snijders JG (1994) *J Chem Phys* 101:9783. doi:[10.1063/1.467943](https://doi.org/10.1063/1.467943)
52. van Lenthe E, van Leeuwen R, Baerends EJ, Snijders JG (1996) *Int J Quantum Chem* 38:2686
53. van Leeuwen R, Baerends EJ (1994) *Phys Rev A* 49:2421. doi:[10.1103/PhysRevA.49.2421](https://doi.org/10.1103/PhysRevA.49.2421)
54. Yang GC, Su ZM, Qin CS (2006) *J Phys Chem A* 110:4817. doi:[10.1021/jp0600099](https://doi.org/10.1021/jp0600099)
55. van Gisbergen SJA, Snijders JG, Baerends EJ (1995) *J Chem Phys* 103:9347. doi:[10.1063/1.469994](https://doi.org/10.1063/1.469994)
56. van Gisbergen SJA, Osinga VP, Gritsenko OV, van Leeuwen R, Snijders JG, Baerends EJ (1996) *J Chem Phys* 105:3142. doi:[10.1063/1.472182](https://doi.org/10.1063/1.472182)
57. van Gisbergen SJA, Snijders JG, Baerends EJ (1996) *Chem Phys Lett* 259:599. doi:[10.1016/0009-2614\(96\)00858-5](https://doi.org/10.1016/0009-2614(96)00858-5)
58. Osinga VP, van Gisbergen SJA, Snijders JG, Baerends EJ (1997) *J Chem Phys* 106:5091. doi:[10.1063/1.473555](https://doi.org/10.1063/1.473555)
59. van Gisbergen SJA, Kootstra F, Schipper PRT, Gritsenko OV, Snijders JG, Baerends EJ (1998) *Phys Rev A* 57:2556. doi:[10.1103/PhysRevA.57.2556](https://doi.org/10.1103/PhysRevA.57.2556)
60. Di Bella S, Fragala I (2002) *N J Chem* 26:285. doi:[10.1039/b201711c](https://doi.org/10.1039/b201711c)
61. Guan W, Yang GC, Yan LK, Su ZM (2006) *Inorg Chem* 45:7864. doi:[10.1021/ic061077c](https://doi.org/10.1021/ic061077c)